SSRG International Journal of Electrical and Electronics Engineering
ISSN: 2348-8379/ https://doi.org/10.14445/23488379/IJEEE-V10I9P118

Volume 10 Issue 9, 190-205, September 2023

Original Article

Deep Learning Approach for the Classification of Caprine Parasites

B. LakshmiNarayana Reddy[1], B. Keerthi Priya[2], K. Rajendra Prasad[3], A.Daisy Rani[4], D.V.Rama Koti Reddy[5]

[1,4,5]*Department of Instrument Technology, Andhra University College of Engineering, Visakhapatnam, Andhra Pradesh, India.*
[2] *Department of Electronics and Communication Engineering, Gayatri Vidya Parishad College of Engineering(A), Visakhapatnam, Andhra Pradesh, India.*
[3]*Department of Computer Science and Engineering, GITAM Deemed to be University, Visakhapatnam, Andhra Pradesh, India.*

[1]*Corresponding Author : dr.adaisyrani@andhrauniversity.edu.in*

Received: 24 July 2023 Revised: 27 August 2023 Accepted: 19 September 2023 Published: 30 September 2023

Abstract *- A parasitic infection is, by far and away, the most common element in animal infectious diseases whose origins may be traced back to most places worldwide. The term "parasite" refers to any organism that lives within another living thing. Because of the near closeness of the people and the animals, there is a danger that the sanitary conditions of the animals will not be adequately treated, which has the potential to have severe ramifications for the health of the people. The surrounding environment has become contaminated due to the spread of parasites and bacteria that dwell in the digestive systems of a wide variety of different animals into the surrounding environment. This has resulted in the contamination of the ecosystem. The main objective of this paper is to employ numerous methods of deep learning to identify the types of parasites found in faeces samples taken from caprine animals. The caprine animals served as the source for the later analyzed samples. Images of parasites such as Amphistome, Ascaris, B-Coli, Moniezia, Schistosoma spindale, Strongyle, and Trichuris are included in the database. These images train and evaluate several models using deep learning techniques such as YOLOv4, YOLOv5, SSD and CNN. The classification results from the study indicate that the YOLOv4 technique can diagnose infections caused by caprine parasites more promptly. This was determined by looking at the results of the performed classification. The fact that the approach produced categorization results provides support for this hypothesis.*

Keywords *- Parasitic worm, Feces, Deep learning, Amphistome, Strongyle, YOLOv5, CNN.*

1. Introduction

The profound connection between people and the animals they have tamed has become even more intimate due to various religious, social, emotional, and physical factors. Cattle and cows are held in high esteem and cherished in several religious traditions originating in India. These traditions include Buddhism, Jainism, and Hinduism. Because there are no known adverse effects and no immediate risk of transmissibility, rumen flukes as a source of nutrition is considered a prevalent practice in the states in the northeastern region of India [1]. Infection can result in a loss of productivity in ruminants, such as a decrease in weight growth or milk production, or a clinical condition, depending on the age of the ruminants, their immune system, and the parasite worms involved. A clinical condition might cause this loss of productivity. The parasitic worms entirely govern this present situation [2].

It is not unusual for dogs and cats to suffer from gastrointestinal parasites, which causes worries in the medical and veterinary communities. Parasites can cause diarrhoea, vomiting, and weight loss in affected animals. These parasites have the potential to bring about both suffering and perhaps death. These parasites can also infect their human hosts, resulting in illness. It is estimated that more than 3 billion people worldwide suffer from parasitic diseases every year [3].

Because of the proximity, there is a significant risk to human health, particularly in circumstances in which the hygienic conditions of the animals are ignored. This risk is exceptionally high when no separation between humans and animals exists. There is a wide variety of parasites that can cause infections. These parasites dwell in the digestive tracts of animals. Helminthes and protozoa are both examples of this group of parasites, which are collectively referred to as the parasite fauna. Helminths can be broken down into two basic phyla; within each phyla, numerous species belong to various families. Nematodes are the most frequent type of helminth that can be transmitted through the soil, and they can be

discovered in the digestive tracts of various animals. In widespread usage, they are also referred to as roundworms rather frequently. The second living organism category is platyhelminths, which are more often referred to as flatworms. They are the most frequent type of flatworm. This category of organisms includes flukes and trematodes in its roster of members [4-5].

Infection occurs via ingesting infective stages such as eggs, larvae, oocysts, or dermal exposure. Infective forms include eggs, larvae, cysts, and oocysts. Oocysts represent a hazardous type of infectious disease. Skin-to-skin contact is the route that accounts for most of all contagious disease transmissions. These virulent forms become particularly significant when animal faeces pollute soil, water, food, and backyards, increasing the chance of interaction between humans and pathogens [6-7].

Amphistomes, also known as stomach flukes or rumen flukes, are the parasites responsible for an illness known as amphistomiasis, which can infect domestic and wild ruminants. Amphistomiasis is a highly lethal condition. Amphistomiasis is a parasitic disease that can be passed on from one host to another. It has been discovered that amphistomes can be found in various organisms, including humans, pigs, horses, and fish. As a result of the failure of the amphistomes to convert nutrients efficiently, the hosts incur a reduction in both their capacity to produce milk and their total body mass [8].

If the eggs of nematode worms belonging to the genus Ascaris are discharged in faeces or deposited in the soil, it is known that they can cause disease in humans, pigs, and horses. These diseases can also be transmitted from soil to animals. Any organism that consumes eggs or vegetation that has eggs on it becomes infected with the parasite, leading to morbidity by inducing intestinal blockage, impairing nutritional status, and disrupting cognitive functions. Eggs and vegetation with eggs on them are both examples of vectors for the parasite. Eggs and vegetation transmit the infection to any organism that eats them [7].

When contaminated food and water are consumed, the intestinal protozoan parasite known as Balantidium coli, which is also referred to as B-coli in some circles, has the potential to transfer from one person to another through the faecal-oral pathway. Chronic diarrhoea, stomach discomfort, and a perforated colon were some of the symptoms the patient had due to the infection caused by B-coli [8].

Moniezia expansa, colloquially known as the ovine tapeworm or the dual-pored ruminant tapeworm, is a parasitic organism inhabiting the small intestines of ruminant animals, including caprine, ovine, and bovine species. The infection may induce host distension, constipation, mild diarrhoea, stunted growth, coarse integument, anaemic conditions, and potential manifestations of mild diarrhoea [9]. Schistosoma spindale is a digenetic trematode species responsible for intestinal schistosomiasis that afflicts ruminants in Sri Lanka, India, Bangladesh, Thailand, Malaysia, and Laos. This condition is known as schistosomiasis. Schistosomiasis, often known as snail fever, is an infection that can either damage the urinary tract or the intestines. This infection can even spread from person to person. This illness can lead to liver damage, kidney failure, infertility, or bladder cancer if left untreated. Other potential complications include infertility [10].

Strongyles are nematode worms that can be found living as parasites in the digestive tracts of mammals such as sheep, horses, and cattle. Strongyles can also be discovered in humans. Nematode worms are what strongyles belong to in the animal kingdom [11]. Trichiuris, more often known as the whipworm, is a parasitic roundworm that infects the large intestine of humans and can potentially cause trichuriasis. Trichiuris can infect other body parts, but the large intestine is its primary host [12].

In clinical parasitology, there is a need for creative diagnostic approaches to solve the obstacles connected with the methods that are currently used to diagnose parasites in animals. Specifically, this need exists to meet the field's demands. The application of deep learning strategies, particularly Convolutional Neural Networks (CNNs), is beneficial in recognizing and categorizing patterns in photographs with relative ease. To facilitate reliable diagnosis of malaria parasites belonging to the genus Plasmodium in patients, CNNs are utilized explicitly for feature extraction from blood smear images [13].

The images are divided into patches and processed by CNNs, employed for three distinct objectives: detecting malaria in dense blood smears, identifying Tuberculosis (TB) bacilli in sputum specimens, and discerning eggs of intestinal parasites within stool samples [14].

After capturing the images, they undergo processing using Convolutional Neural Networks (CNNs) to accomplish three distinct tasks. Firstly, the CNN is utilized to ascertain the existence of malaria within dense blood smears. This crucial task involves analyzing the images of the blood samples and identifying the characteristic signs of malaria parasites.

Secondly, the CNN plays a vital role in diagnosing Tuberculosis Bacillus (TB) in sputum specimens. By carefully analyzing the images, CNN assists in identifying the presence of TB bacteria, aiding in the accurate diagnosis of this infectious disease. Lastly, the CNN is employed to identify intestinal parasite eggs from stool samples, ensuring effective and efficient detection of these harmful parasites. To enable the completion of these tasks, the photos are initially divided or split into smaller patches for further analysis and interpretation by the CNN.

LSTM is used to detect Tuberculosis (TB) from 1265 microscopy pictures and sputum samples. LSTM recurrent neural networks interpret sequential data well, making them suitable for time series problems. The LSTM architecture analyses microscope pictures of the sputum samples to categorize them as TB-positive or negative. This concept promises accurate and automated Tuberculosis (TB) detection, improving diagnosis and treatment [15]. Contrast Limited Adaptive Histogram Equalisation (CLAHE) uses cutting-edge technology to improve blood stain pictures and TB detection. CLAHE enhances contrast and reveals small details by adjusting the histogram. CLAHE intends to highlight TB-related traits in blood smear images. This method could improve TB detection and treatment [16].

The authors used Inception V3 and Xception CNN architectures and a voting-based ensemble approach. CNN models segmented microscopic pictures to identify parasite egg species and count faeces eggs automatically. Ensemble learning and advanced CNN architectures improve diagnostic parasite detection and egg quantification [17, 18]. Narut et al. classified Ascaris lumbricoides eggs from stool samples using CNN architecture with 93.33 percent accuracy. Parra et al. [19] employed image processing to identify parasites in reptile excrement using CLAHE and OTSU. They used a convolutional network with MobileNet architecture and a Single-Shot multibox Detector (SSD). These methods use CNNs and image processing to detect and identify parasites in various sample types, improving diagnostic capabilities.

This study aims to detect faeces parasites, including Amphistome, Ascaris, B-Coli, Moniezia, Schistosoma spindale, Strongyle, and Trichuris. Examining parasite ova spread on glass slides with an Olympus microscope is part of the investigation. Through microscopy, 84 images representing seven distinct parasites are obtained. These images are then classified using deep-learning networks like CNN, SSD, YOLOv4, and YOLOv5. This research is one of the first in India to employ deep learning methodologies for identifying and classifying caprine parasites, demonstrating the innovative use of these technologies in veterinary diagnostics.

2. Materials and Methods

2.1. Sample Preparation and Image Acquisition

Faecal examination is a widely used method to detect various gastrointestinal parasites in cattle. The process involves collecting animal faecal samples and promptly preserving them at 2 to 8°C. The samples are then subjected to the formalin-ether concentration technique, which concentrates parasite ova and cysts. The resulting sediment is then spread on a clean glass slide to analyze further and identify the parasites. This approach enables the effective detection and characterization of gastrointestinal parasites in cattle through microscopic examination [22]. Under the supervision of experts, Sri Venkateswara Veterinary University in Tirupati prepares samples for examination. The specimens are analyzed using a digital biological microscope, the Olympus CX43 microscope. This user-friendly microscope enables specimen manipulation with one hand while focus adjustment and operation are performed with the other, minimizing the need for physical movement. The microscope has an integrated Kohler illumination system with a 2.4W Light-Emitting Diode (LED) for adequate illumination.

The microscope also includes an optional camera interface for digital imaging. A Magnus CMOS 5MP C-Mount camera with USB connectivity is used for image acquisition. Compatible with both binocular and trinocular versions of sophisticated microscopes, the camera has a maximum resolution of 2592 x 1944 pixels. Figure 1 displays an Olympus CX43 microscope, a Magnus digital camera, and an image of a parasite extracted from a faecal B-coli sample. As depicted in Figure 1, the glass plates can be observed in their natural colours due to the LED illumination.

(a)

(b)

Fig. 1 Images of microscope and camera (a) Olympus CX43 microscope, and (b) Magnus 5MP CMOS digital camera.

To conduct the analysis, specialists at the veterinary university collected and visually annotated all digital images containing any parasite. Seven categories of parasites were represented by 650 images from various samples: Amphistome, Ascaris, B-Coli, Moniezia, Schistosoma spindale, Strongyle, and Trichuris. This extensive dataset enables a thorough examination and classification of different parasite species included in the study.

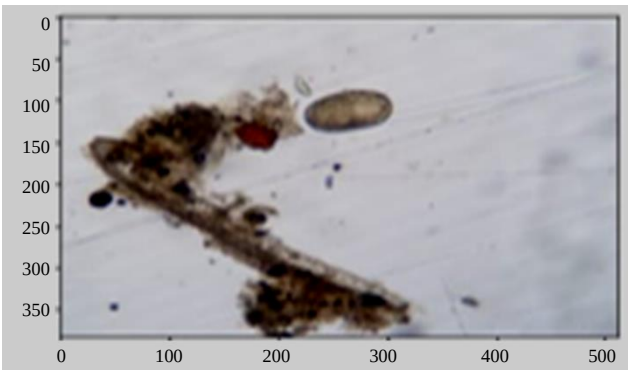

(a)

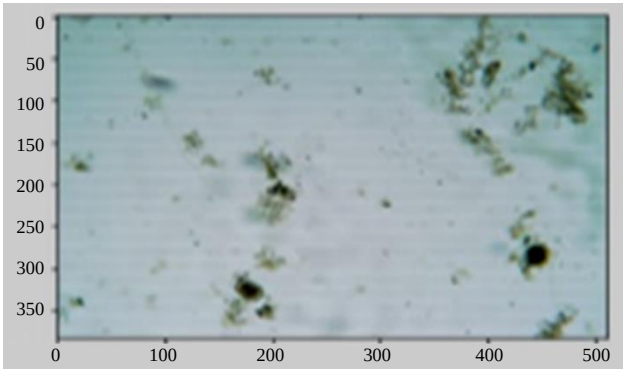

(b)

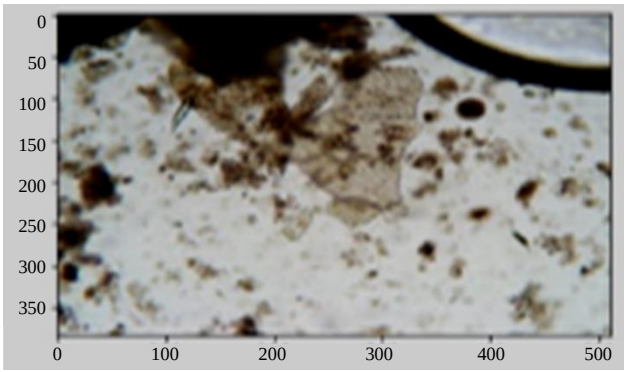

(c)

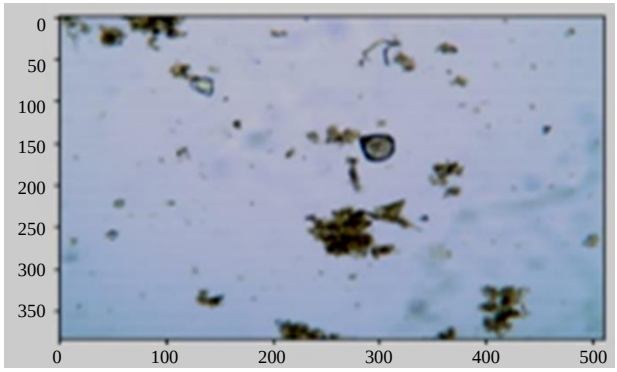

(d)

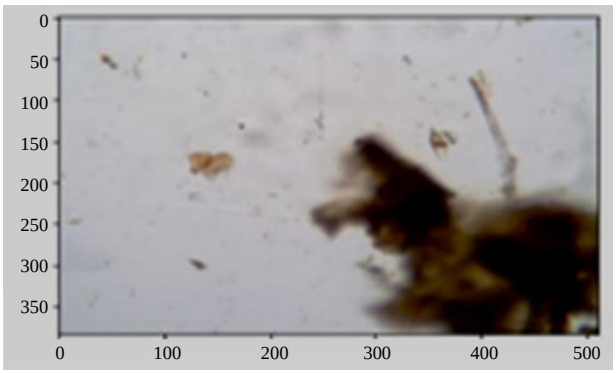

(e)

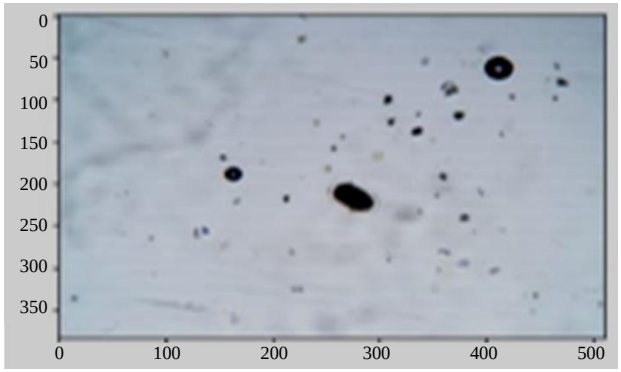

(f)

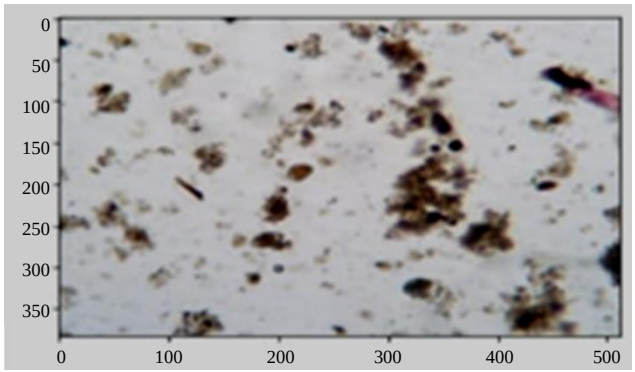

(g)

Fig. 2 Images of the parasites (a) Amphistome, (b) Ascaris, (c) B-Coli, (d) Moniezia ova, (e) Schistosoma spindale, (f) Strongyle eggs, and (g) Trichuris eggs.

2.2. Deep Learning Techniques

After obtaining the microscopic images, the next stage is to analyze them to determine the specific parasite species. This is accomplished by training a CNN with annotated image data. The training process entails deriving features from the labelled training data to enable the network to recognize various parasite species. Upon successful training and validation of the CNN model, novel data inputs can be introduced to the network, yielding delineated segmentation outcomes and labelled parasite delineations [17]. CNN functions by segmenting the image into regions and predicting boundary boxes alongside associated probabilities for each distinct

region. Concurrently, it can predict numerous bounding boxes and corresponding possibilities for diverse categories of parasites, thereby enhancing the precision of the detection process.

The Convolutional Neural Network (CNN) outperforms other network architectures with image, audio, or speech inputs. As shown in Figure 3, CNNs consist of critical components: the convolutional, pooling and Fully-Connected (FC) layers, forming a fundamental architecture. These layers allow CNN to effectively analyze and extract features from input data, making it ideally suited for tasks involving visual and aural data.

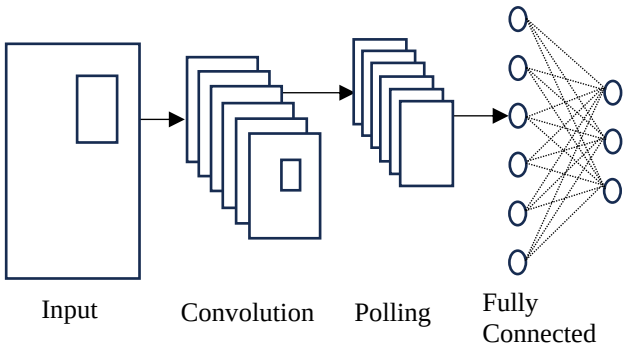

Fig. 3 The main components of convolutional neural network

The basic convolutional layer, which serves as the groundwork for sophisticated computations, is at the heart of CNNs. Following each convolutional operation, incorporating a Rectified Linear Unit (ReLU) transformation injects crucial nonlinearity into the resulting feature map, enhancing the network's potential for subtle pattern detection and extraction.

Pooling layers, also known as downsampling layers, are essential in dimensionality reduction by mitigating the risk of overfitting, increasing efficiency, and decreasing complexity. The max pooling approach systematically determines the pixel with the most outstanding value within specified regions, encapsulating the most significant degree of feature representation. The average pooling technique, on the other hand, performs a rigorous computation by computing the arithmetic mean of pixel values inside the defined zones, providing a complete overview of feature content. The Fully-Connected (FC) layer executes the classification task using the parameters extracted from previous layers.

The FC layer is typically outfitted with a softmax activation mechanism, customized to optimize the classification process, emphasizing heightened accuracy and discernment. While convolutional and pooling layers can be layered, an FC layer is often the concluding layer. With the addition of each layer, the network's complexity increases, enabling the identification of more significant portions of the input image, resulting in enhanced feature extraction and classification capabilities. The SSD is an exemplary object detection method that utilizes the multi-box approach to accurately detect and locate many items in a single computing pass. SSD detects multiple objects with a single deep neural network and achieves exceptional speed and accuracy [20]. In classifying reptile parasites [19], an SSD-based object detection network is utilized. This SSD network is built on a feed-forward CNN and generates fixed-size bounding boxes and scores indicating parasite class instances within those boxes [20].

SSD is renowned for its exceptional speed and high-precision object detection capabilities. This is made possible by two essential factors. SSD eliminates the need for bounding box proposals, resulting in a more streamlined and effective process. Second, it utilizes convolution filters that predict both the categories of parasites and the offsets for bounding box locations. In subsequent phases, these extracted filters can be applied to multiple feature maps, enabling detection at various scales. Figure 4 depicts the operation of parasite diagnosis utilizing the SSD algorithm, demonstrating its capacity to detect and classify parasites based on these principles efficiently. Due to its speed and precision, SSD is a valuable tool for object detection duties, including parasite diagnosis.

The VGG-16 network is used to derive feature maps from the input image of a parasitic worm. Six convolutional layers are then applied to these extracted feature maps to classify the image. The SSD algorithm generates 8732 predictions for bounding boxes with varied aspect ratios. The output of the images is determined using the IOU (Intersection Over Union) technique by selecting the frames with the most significant overlap. This method facilitates the identification and localization of objects, in this case, the parasitic worm, by generating multiple predictions and refining them according to the degree of overlap.

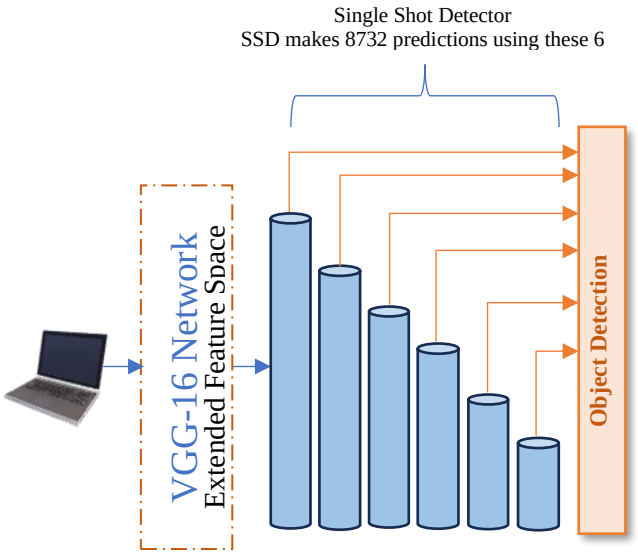

Fig. 4 Implementation of SSD for diagnosis of caprine parasites

The YOLO algorithm is designed to perceive and classify objects in images in real time. It employs a novel methodology to address the complex challenge of object detection by framing it as a regression problem. As a result, it provides valuable probability predictions for the various classes of the detected items. [22].

For efficient real-time object detection, the algorithm employs a CNN, with the Darknet functioning as the underlying backbone network. YOLOv4, proposed by Alexy et al. in 2020, is a cutting-edge real-time object detection model with extensive applications in computer vision tasks, such as unmanned driving [24, 25]. YOLOv5, on the other hand, is extensively used as a single-stage anchor-based object detector due to its rapid training speed and simple deployment support. This study concentrates on YOLOv4 and YOLOv5, even though there are multiple versions of YOLO.

The YOLO real-time object recognition framework outperforms contemporary methods in precision and speed. It can distinguish and classify several items in a single frame. The distinguishing feature of YOLO is its ability to exploit the totality of an image throughout the processes of both training and assessment, allowing the implicit storing of extensive contextual elements about various classes and their exhibited appearances. Numerous accurate object detection models necessitate using multiple GPUs for training with enormous mini-set sizes. Nevertheless, training such prototypes with a single GPU is impractical and time-consuming.

To counter this challenge, YOLOv4 employs a strategic approach by formulating an object detection system that exhibits optimized trainability on a singular GPU, achieved through the utilization of a diminished minibatch size. This method facilitates the training of a super-fast, precise object detector using the CSPDarknet53 model as the GPU version's feature extractor. The model is underpinned by Darknet, a meticulously engineered open-source neural network framework coded in C and CUDA. This foundation is the cornerstone upon which the model's intricate architecture and functionality are precisely constructed and executed. It comprises 53 convolutional layers intimately linked to both batch normalization and Mish activation layers.

YOLOv5 similarly circumvents the GPU limitation by employing a reduced mini-batch size. It utilizes ConvNet as the network's backbone, facilitating the transformation of one part of initiations to another via a differentiable function. By decreasing the mini-batch size, YOLOv5 can circumvent the GPU limitation and accomplish efficient training.

3. Results and Discussion

Table 1 summarises the deep learning techniques used in this study, highlighting their respective characteristics.

Table 1. Characteristics of deep learning networks used to detect caprine parasitic worms

Parameter	CNN	SSD	YOLO v5	YOLO v4
Training Time	30 min	5 h	30 min	2 h 30 min
Detection Speed	25 sec	2-3sec	4 seconds	4 sec
Accuracy	70-90%	75-85%	85-95%	90-98%
Layers	3 layers	6 layers	4 Fusion layers	53 Conv layers
Mean Average Precision (MAP)	0.76	0.251	0.98	0.358
Frames per Second	No frames	59	140	45

Examining Table 1 and Figure 5, it is evident that every network has its benefits and drawbacks. CNN, unlike other networks, has no specific data format requirements. SSD requires five hours of training, while CNN and YOLOv5 only need thirty minutes. YOLOv4 is a more complex network with 53 convolution layers, whereas CNN operates with a smaller image dimension of 150x150 pixels. SSD has a mean average precision of 0.251, whereas YOLOv5 achieves 0.98. YOLO stands out regarding frames computed per second, as YOLOv4 can handle 45 frames, whereas YOLOv5 can handle 140 structures in the same time frame. Regarding dataset compatibility, training time, model complexity, precision, and processing speed, these performance characteristic variances emphasize each network's unique attributes.

Table 2 compares the efficacy of the discussed architectures based on their respective precision values. It enables investigators and researchers to evaluate and prefer the most pertinent architecture based on their needs. YOLOv4 and YOLOv5 improve real-time object detection by addressing the GPU limitation and optimizing the training process. These architectures facilitate accurate and efficient object recognition by leveraging cutting-edge models like CSPDarknet53 and ConvNet. The availability of accuracy values in Table 2 enables the selection of an appropriate architecture for object detection tasks.

CNN achieves 86% accuracy in Amphistome detection, YOLOv4 achieves 100%, and YOLOv5 achieves 92%. In diagnosing Ascaris eggs, YOLOv4 exceeds YOLOv5 and CNN, with an accuracy of 98%, whereas YOLOv5 reaches 82% and CNN achieves 73%. YOLOv5 and CNN, on the other hand, struggle to detect B-Coli, with accuracies of 34% and 53%, respectively, but YOLOv4 excels with 99% accuracy.

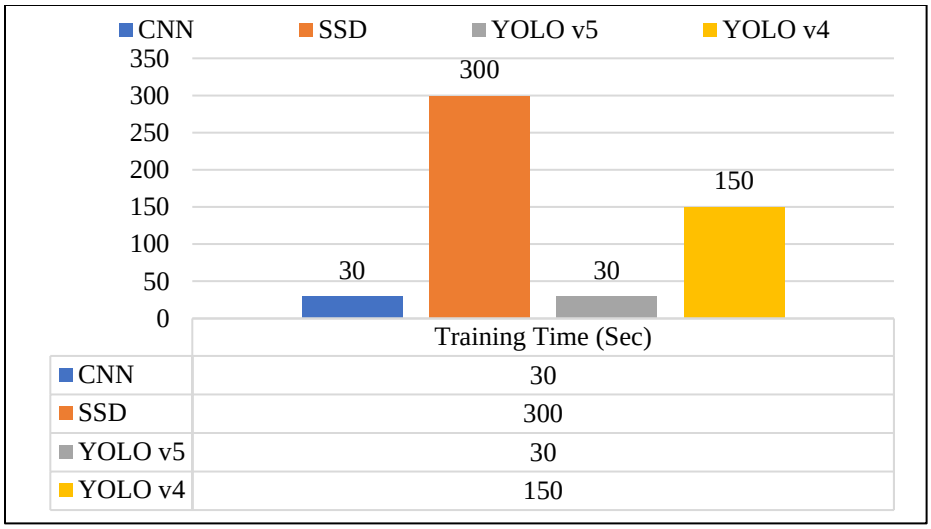
CNN
SSD
YOLO v5
YOLO v4
350
300
250
200
150
100
50
0
30
300
30
150
Training Time (Sec)
CNN 30
SSD 300
YOLO v5 30
YOLO v4 150

(a)

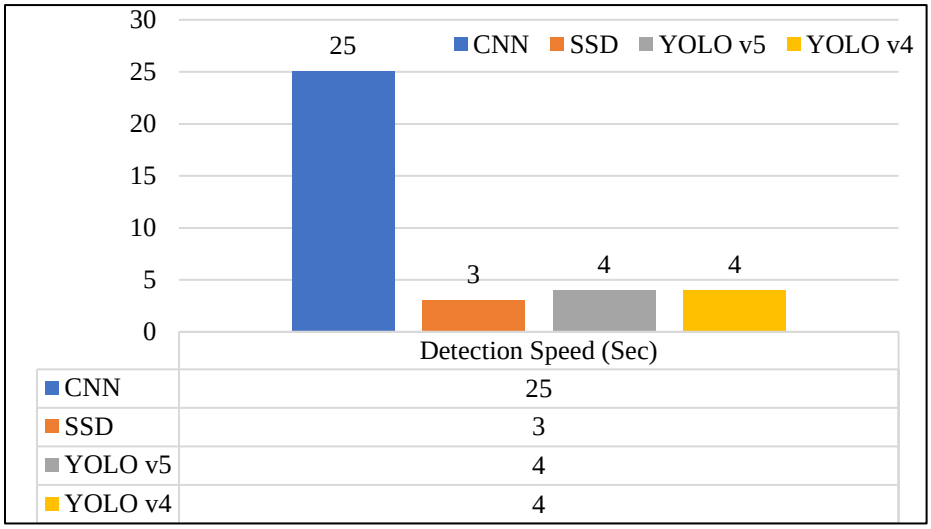
30
25
20
15
10
5
0
25
3
4
4
CNN
SSD
YOLO v5
YOLO v4
Detection Speed (Sec)
CNN 25
SSD 3
YOLO v5 4
YOLO v4 4

(b)

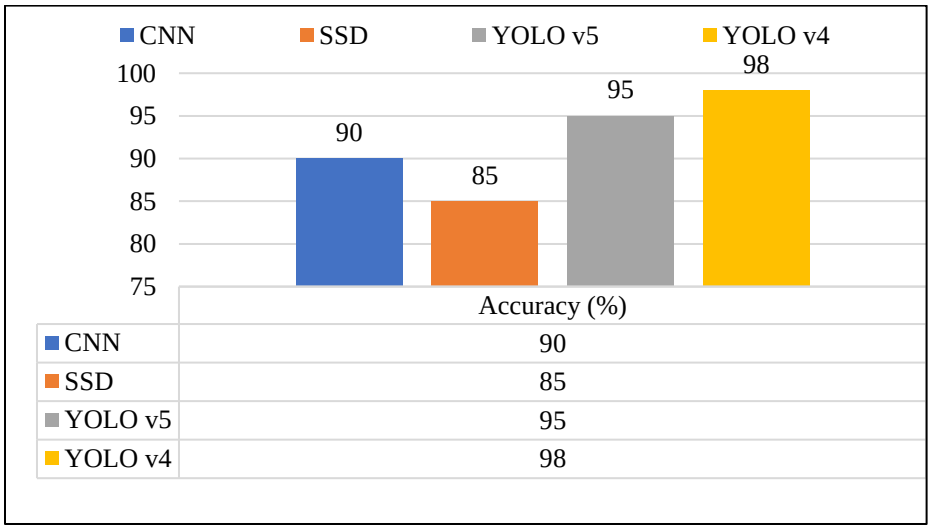
CNN
SSD
YOLO v5
YOLO v4
100
95
90
85
80
75
90
85
95
98
Accuracy (%)
CNN 90
SSD 85
YOLO v5 95
YOLO v4 98

(c)

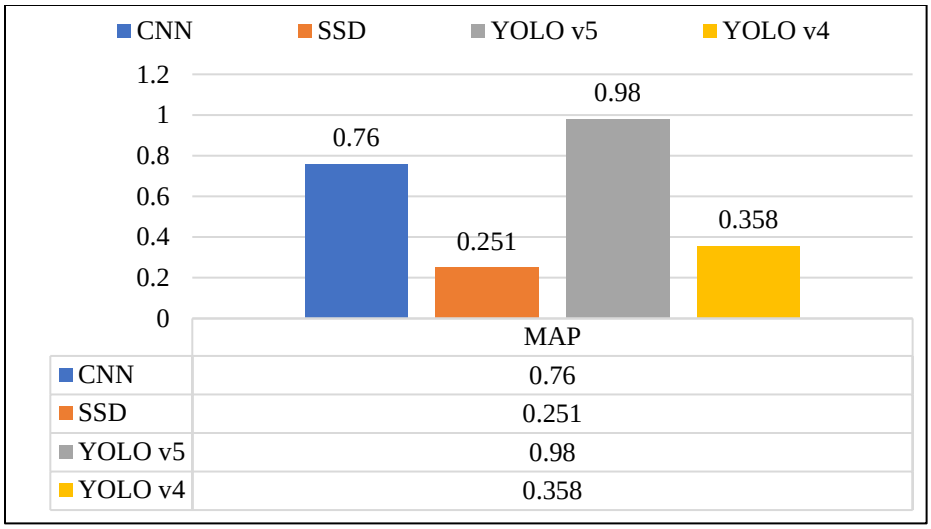

(d)

Fig. 5 Bar Plots of a) Training time, b) Detection speed, c) Accuracy, and d) Mean precision average.

Table 2. Classification accuracy values obtained from CNN, YOLO v4 and YOLO sv5 networks (in %)

Parasite Type	CNN	YOLO v5	YOLO v4
Amphistome	86	92	99
Ascaris	73	82	98
B-Coli	53	34	99
Moniezia	84	89	99
Schistosoma Spindale	84	87	98
Strongyle	79	80	92
Trichuris	91	52	91

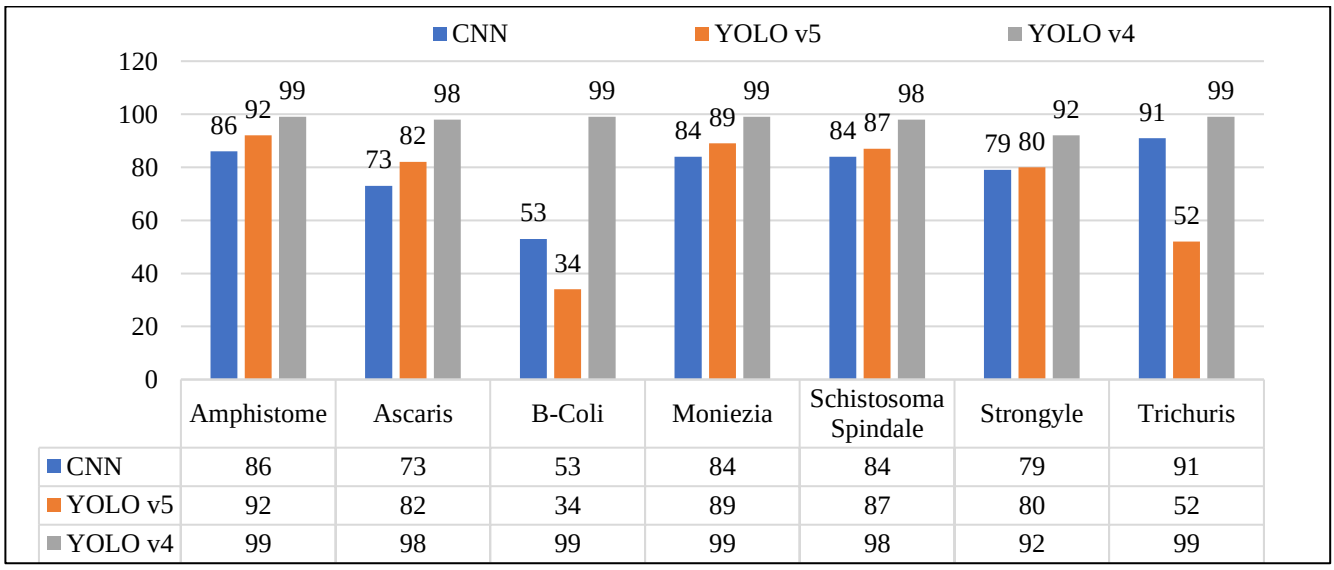

Fig. 6 Bar plot of accuracy values obtained from CNN, YOLO v5, and YOLO v4

```
[yolo] params: iou loss: ciou (4), iou_norm: 0.07, obj_norm: 1.00, cls_norm: 1.00, delta_norm: 1.00, scale_x_y: 1.05
nms_kind: greedynms (1), beta = 0.600000
Total BFLOPS 6.797
avg_outputs = 300464
 Allocate additional workspace_size = 12.46 MB
Loading weights from darknet/backup/yolov4-custom_last.weights...
 seen 64, trained: 416 K-images (6 Kilo-batches_64)
Done! Loaded 38 layers from weights-file
 Detection layer: 30 - type = 28
 Detection layer: 37 - type = 28
darknet/images/Amphistome_11.jpg: Predicted in 15.652000 milli-seconds.
amphistone: 100%
Unable to init server: Could not connect: Connection refused

(predictions:1662): Gtk-WARNING **: 14:18:22.346: cannot open display:
```

a) Output of Amphistome with 99% accuracy

```
[yolo] params: iou loss: ciou (4), iou_norm: 0.07, obj_norm: 1.00, cls_norm: 1.00, delta_norm: 1.00, scale_x_y: 1.05
nms_kind: greedynms (1), beta = 0.600000
Total BFLOPS 6.797
avg_outputs = 300464
 Allocate additional workspace_size = 12.46 MB
Loading weights from darknet/backup/yolov4-custom_last.weights...
 seen 64, trained: 416 K-images (6 Kilo-batches_64)
Done! Loaded 38 layers from weights-file
 Detection layer: 30 - type = 28
 Detection layer: 37 - type = 28
darknet/images/Ascaris.jpg: Predicted in 15.638000 milli-seconds.
ascaris_egg: 96%
ascaris_egg: 98%
Unable to init server: Could not connect: Connection refused

(predictions:1686): Gtk-WARNING **: 14:20:07.351: cannot open display:
```

b) Output of Ascaris egg with 98% accuracy

```
[yolo] params: iou loss: ciou (4), iou_norm: 0.07, obj_norm: 1.00, cls_norm: 1.00, delta_norm: 1.00, scale_x_y: 1.05
nms_kind: greedynms (1), beta = 0.600000
Total BFLOPS 6.797
avg_outputs = 300464
 Allocate additional workspace_size = 12.46 MB
Loading weights from darknet/backup/yolov4-custom_last.weights...
 seen 64, trained: 416 K-images (6 Kilo-batches_64)
Done! Loaded 38 layers from weights-file
 Detection layer: 30 - type = 28
 Detection layer: 37 - type = 28
darknet/images/BColi.jpg: Predicted in 15.656000 milli-seconds.
b_coli: 78%
b_coli: 99%
Unable to init server: Could not connect: Connection refused

(predictions:1710): Gtk-WARNING **: 14:21:27.695: cannot open display:
```

c) Output of B-Coli with 99% accuracy

```
[yolo] params: iou loss: ciou (4), iou_norm: 0.07, obj_norm: 1.00, cls_norm: 1.00, delta_norm: 1.00, scale_x_y: 1.05
nms_kind: greedynms (1), beta = 0.600000
Total BFLOPS 6.797
avg_outputs = 300464
 Allocate additional workspace_size = 12.46 MB
Loading weights from darknet/backup/yolov4-custom_last.weights...
 seen 64, trained: 416 K-images (6 Kilo-batches_64)
Done! Loaded 38 layers from weights-file
 Detection layer: 30 - type = 28
 Detection layer: 37 - type = 28
darknet/images/Moneizia_Ova_Egg_04.jpg: Predicted in 15.678000 milli-seconds.
moneizia_ova: 99%
Unable to init server: Could not connect: Connection refused

(predictions:1732): Gtk-WARNING **: 14:22:18.813: cannot open display:
```

d) Output of Moneizia ova with 99% accuracy

```
[yolo] params: iou loss: ciou (4), iou_norm: 0.07, obj_norm: 1.00, cls_norm: 1.00, delta_norm: 1.00, scale_x_y: 1.05
nms_kind: greedynms (1), beta = 0.600000
Total BFLOPS 6.797
avg_outputs = 300464
 Allocate additional workspace_size = 12.46 MB
Loading weights from darknet/backup/yolov4-custom_last.weights...
 seen 64, trained: 416 K-images (6 Kilo-batches_64)
Done! Loaded 38 layers from weights-file
 Detection layer: 30 - type = 28
 Detection layer: 37 - type = 28
darknet/images/Schistosoma_Spindale_01.jpg: Predicted in 16.044000 milli-seconds.
schistosoma_spindale: 100%
Unable to init server: Could not connect: Connection refused

(predictions:1756): Gtk-WARNING **: 14:23:16.686: cannot open display:
```

e) Output of Schistoma spindale with 98% accuracy

```
[yolo] params: iou loss: ciou (4), iou_norm: 0.07, obj_norm: 1.00, cls_norm: 1.00, delta_norm: 1.00, scale_x_y: 1.05
nms_kind: greedynms (1), beta = 0.600000
Total BFLOPS 6.797
avg_outputs = 300464
 Allocate additional workspace_size = 12.46 MB
Loading weights from darknet/backup/yolov4-custom_last.weights...
 seen 64, trained: 416 K-images (6 Kilo-batches_64)
Done! Loaded 38 layers from weights-file
 Detection layer: 30 - type = 28
 Detection layer: 37 - type = 28
darknet/images/Strongyle_02.jpg: Predicted in 15.792000 milli-seconds.
strongyle: 92%
Unable to init server: Could not connect: Connection refused

(predictions:1808): Gtk-WARNING **: 14:26:25.559: cannot open display:
```

f) Output of Strongyle egg with 92% accuracy

```
[yolo] params: iou loss: ciou (4), iou_norm: 0.07, obj_norm: 1.00, cls_norm: 1.00, delta_norm: 1.00, scale_x_y: 1.05
nms_kind: greedynms (1), beta = 0.600000
Total BFLOPS 6.797
avg_outputs = 300464
 Allocate additional workspace_size = 12.46 MB
Loading weights from darknet/backup/yolov4-custom_last.weights...
 seen 64, trained: 416 K-images (6 Kilo-batches_64)
Done! Loaded 38 layers from weights-file
 Detection layer: 30 - type = 28
 Detection layer: 37 - type = 28
darknet/images/Trichuris_Egg_16.jpg: Predicted in 15.842000 milli-seconds.
trichuris_egg: 100%
Unable to init server: Could not connect: Connection refused

(predictions:1828): Gtk-WARNING **: 14:27:21.134: cannot open display:
```

g) Output of Trichuris egg with 99% accuracy

Fig. 7 Classification results obtained using YOLOv5 for parasites

a) Output of Amphistome with 0.92 accuracy

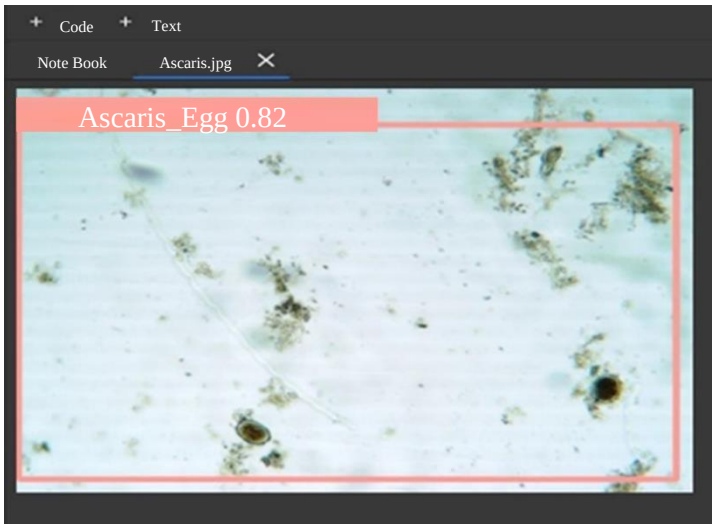

b) Output of Ascaris egg with 0.82 Accuracy

c) Output of Moneizia ova with 0.89 Accuracy

d) Output of Strongyle egg with 0.80 Accuracy

Fig. 8 Classification results obtained using YOLO v5 for parasites

In the case of Moniezia Ova Eggs, CNN and YOLOv5 perform similarly, with 84% and 89% accuracy, respectively. For Moniezia Ova Eggs and Trichuris Eggs, YOLOv5 has the highest accuracy. CNN obtains 79% accuracy for Strongyle eggs, YOLOv4 reaches 92%, and YOLOv5 achieves 80%. Based on the accuracy values shown in Table 2 and Figure 6, it is clear that YOLOv4 is the most efficient network for parasitic worm detection, consistently achieving high accuracy across diverse egg types. To thoroughly evaluate the accuracy values, it is necessary to consider network characteristics such as architecture design, training methods, and specific features used. Other criteria, including computing needs, training time, and practical deployment, should also be considered when selecting the best network for parasite detection tasks. A more comprehensive understanding of parasite detection and identification can be obtained by correlating accuracy with network properties. Figure 7 displays the research findings obtained using YOLOv4 to classify parasitic worms. Figure 8 displays the experimental results obtained using YOLO v5 to classify parasitic worms. Figure 9 displays the experimental results obtained using CNN to classify parasitic worms.

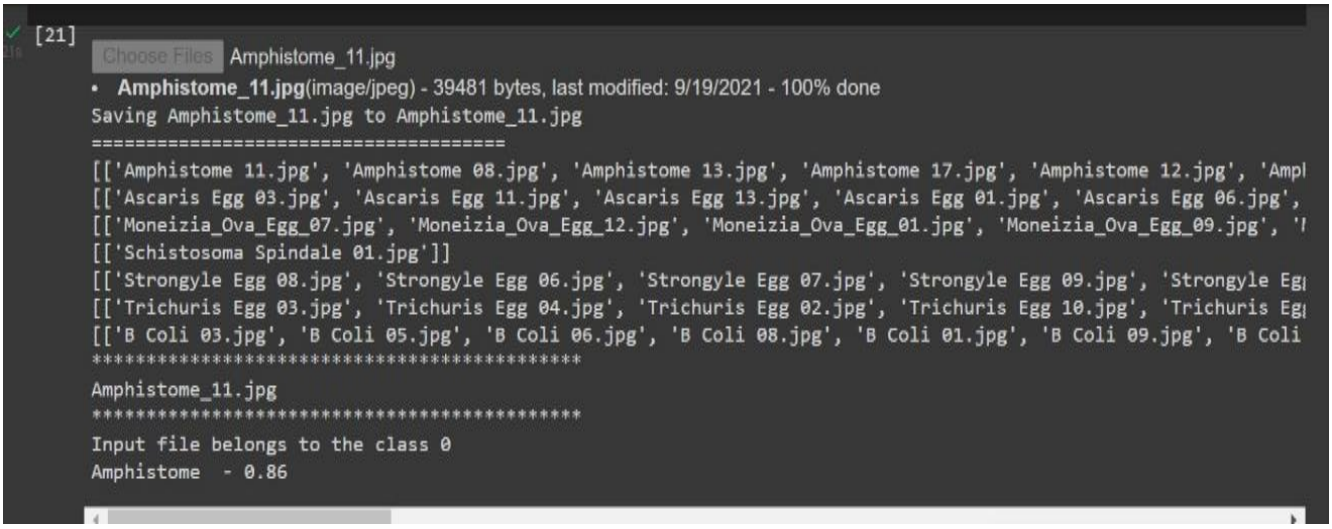

a) Output of Amphistome with 86% accuracy

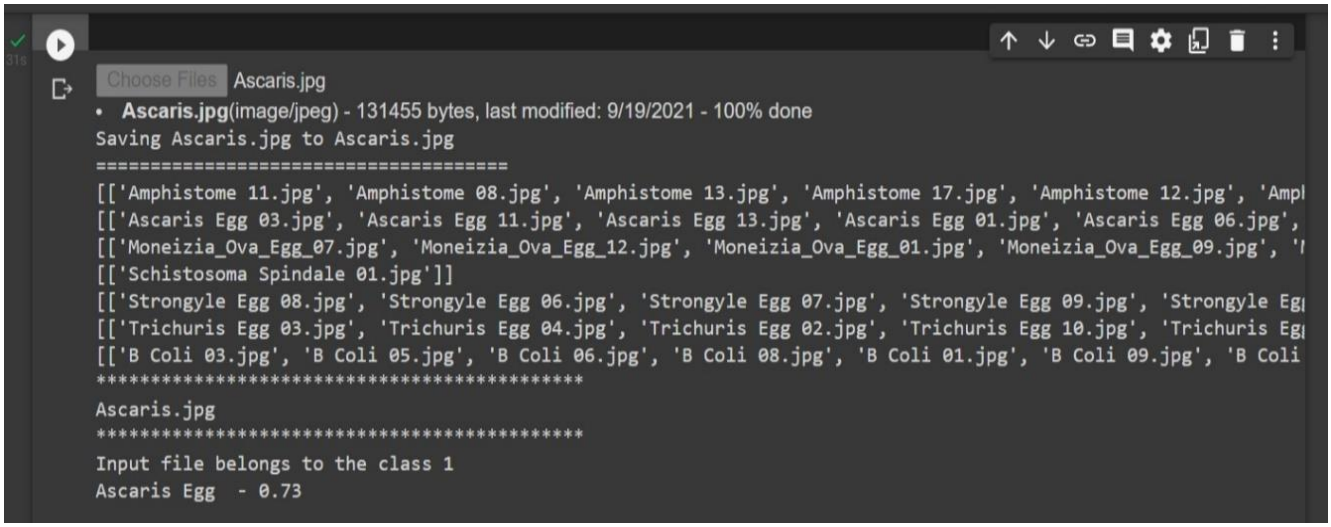

b) Output of Ascaris egg with 73% accuracy

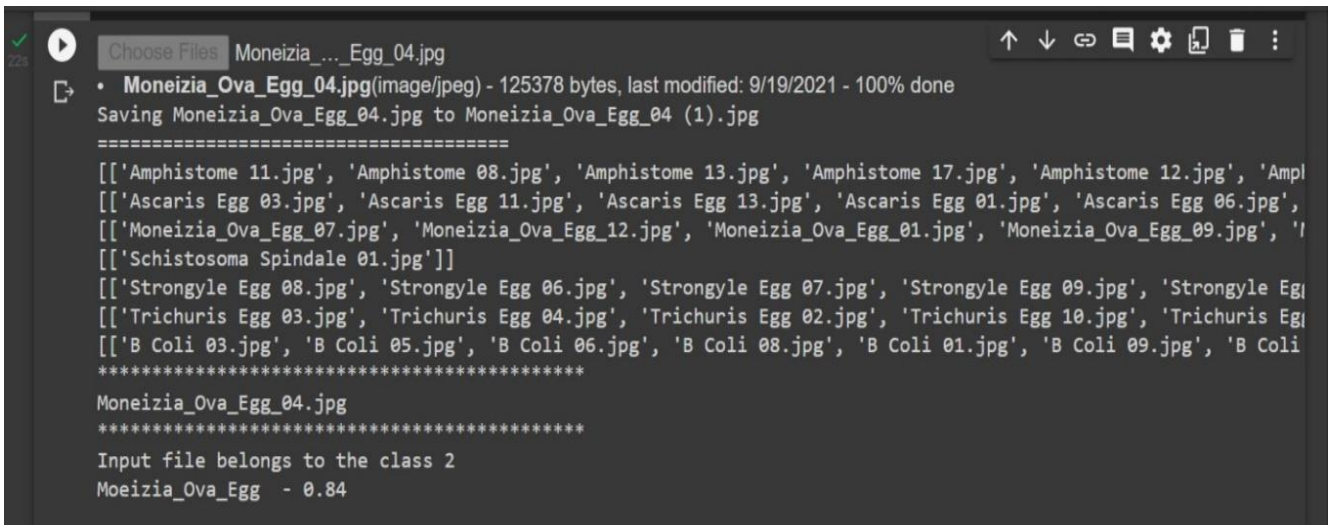

c) Output of Moneizia ova with 84% accuracy

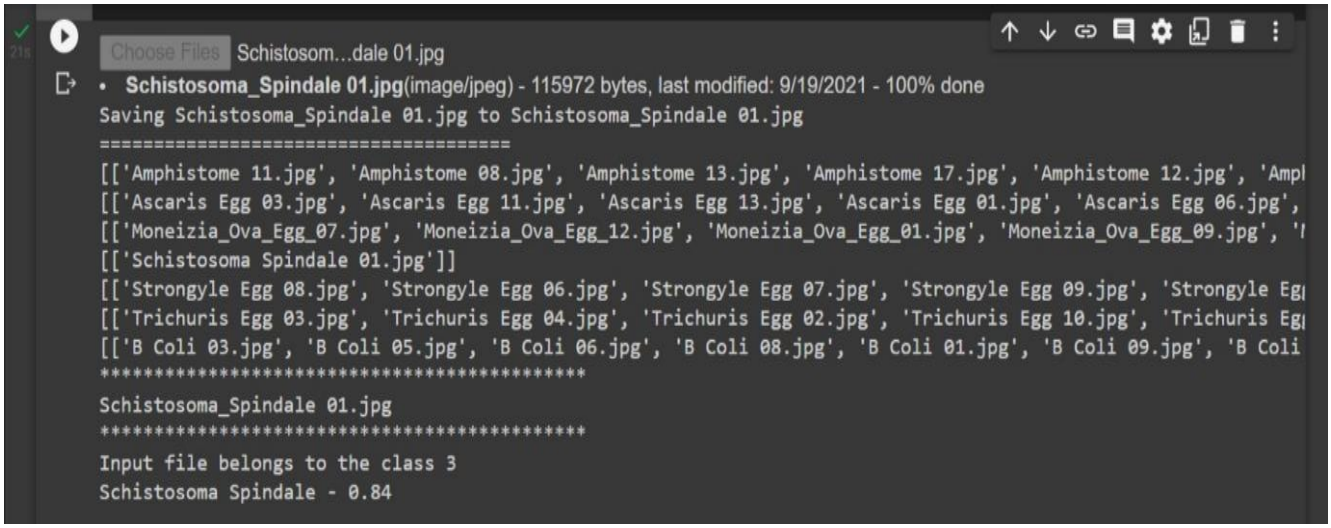

d) Output of the Schistoma spindale with 84% accuracy

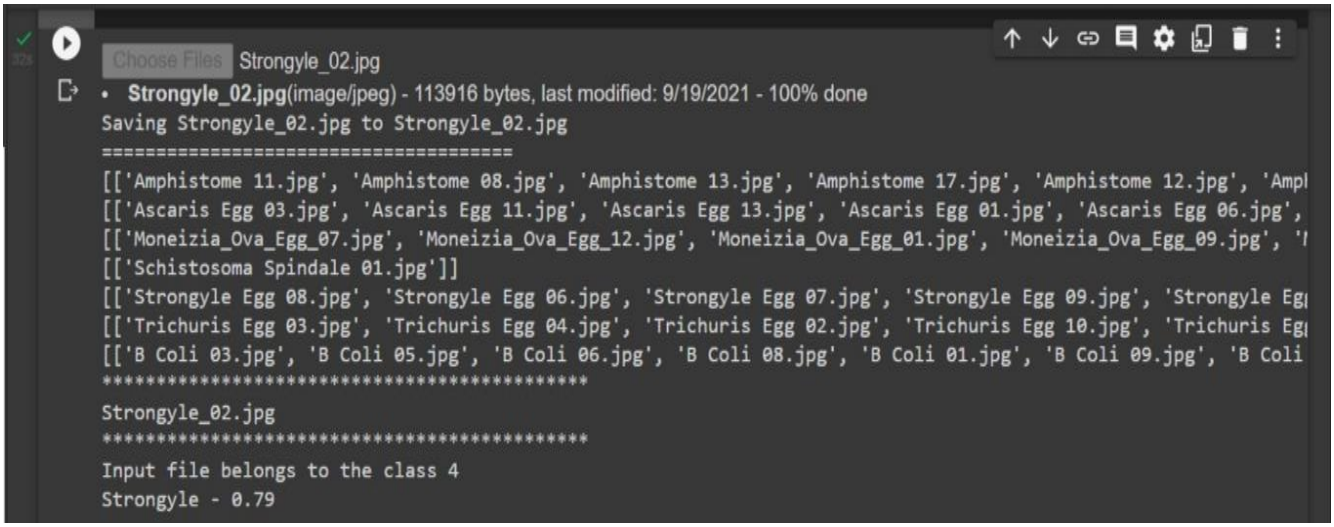

e) Output of Strongyle egg with 79% accuracy

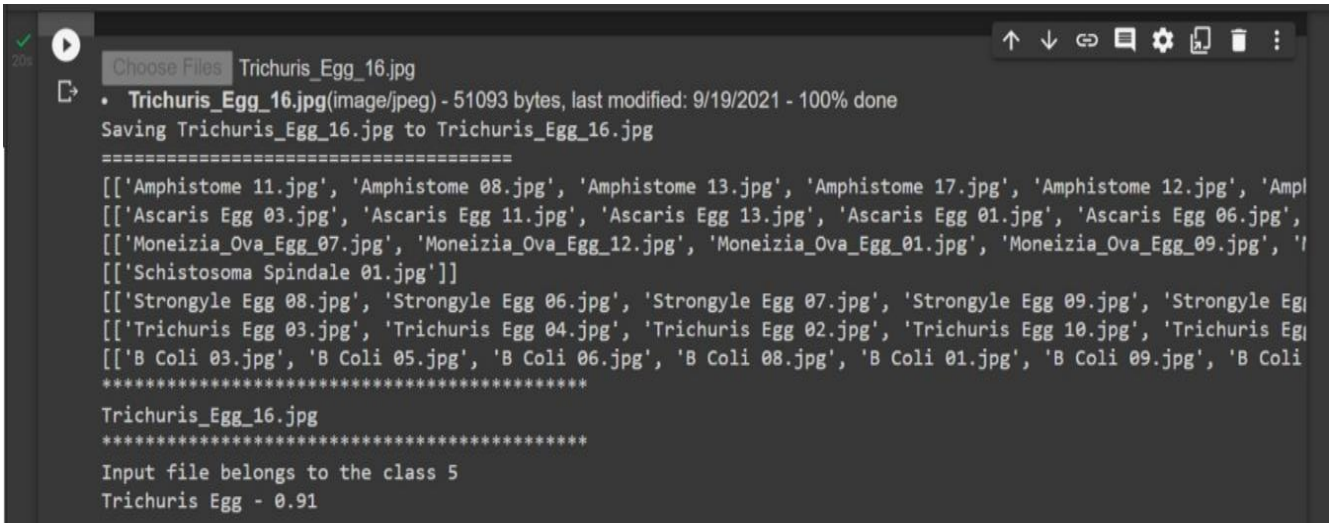

f) Output of Trichuris egg with 91% accuracy

Fig. 9 Classification results obtained using CNN for parasites

The present study has demonstrated the detection of different parasites in Indian livestock using deep learning techniques. The limitations in detecting parasites reported in the study may be attributed to inexperienced staff at the diagnostic sites who are less familiar with the uncommon parasites. The clinical signs of infection caused by Schistosoma are rarely seen in Indian cattle, and their focus may be on detecting other flukes. This may result in negligence in detecting the parasites (Schistosoma). Similarly, the experts also underestimated Amphistomiasis caused by the parasite amphistomes. The trematode Schistosoma spindale co-occurs with other gastrointestinal parasites such as Strongyle. Less literature is available on the infection of B-coli in humans and cattle. There is a need to analyze under-estimated and common parasites, so it is prudent to detect more parasites simultaneously.

Furthermore, the study demonstrates how deep learning algorithms can be implemented to detect caprine parasites. A high accuracy of 100% was achieved for detecting Amphistome, Schistosoma spindale and Trichuris on a small test set of images using the YOLOv4 network. YOLOv5 is faster, user-friendly and not as complex as other networks, even though the performance is less compared to YOLOv4. It is not feasible to conclude that YOLOv4 is the best network for classifying caprine parasites based on a single performance metric.

Different performance metrics will be considered on a large set of test image data in the future. Recently, deep learning-based approaches for detecting parasites have attracted substantial attention due to their high performance in different image classification tasks. These techniques incorporate faster diagnosis of parasite infection and somewhat resolve the lack of skilled persons.

4. Conclusion

The present work aims to deploy deep learning techniques in detecting caprine parasites. The digital images of faecal samples collected from the Sri Venkateswara Veterinary University, Tirupati, are analyzed for this purpose. Six hundred fifty pictures of seven different parasites named Amphistome, Ascaris, B-Coli, Moniezia, Schistosoma spindale, Strongyle, and Trichuris are used. The deep learning networks tested in the study are the CNN, SSD, YOLOv4 and YOLOv5. The YOLOv4 network achieved classification accuracy of 98% for detecting Amphistome, Schistosoma spindale and Trichuris. In subsequent investigation, different performance metrics will be analyzed on extensive data for more reliable detection of caprine parasites. The proposed technique is used for faster diagnosis of parasitic infection and is expected to replace the lack of skilled experts to some extent.

Acknowledgments

The authors express heartfelt gratitude to Professor Chengalvarayulu, the distinguished former Head of the Parasitology Department, for his generous provision of invaluable digital faecal sample images collected from Sri Venkateswara Veterinary University, Tirupati. His noteworthy contribution has significantly enhanced the comprehensiveness and profundity of research pursuits, illuminating pivotal facets of the investigation and propelling progress in the field of veterinary sciences.

References

[1] P.C. Sarmah et al., "Human Consumption of Rumen Flukes of Cattle in India," *Southeast Asian Journal of Tropical Medicine and Public Health*, vol. 45, no. 1, pp. 26-30, 2014. [Google Scholar] [Publisher Link]

[2] Johannes Charlier et al., "Chasing Helminths and their Economic Impact on Farmed Ruminants," *Trends in Parasitology*, vol. 30, no. 7, pp. 361-367, 2014. [CrossRef] [Google Scholar] [Publisher Link]

[3] Pinar Okyay et al., "Intestinal Parasites Prevalence and Related Factors in School Children, a Western City Sample - Turkey," *BMC Public Health*, vol. 4, no. 64, pp. 1-6, 2004. [CrossRef] [Google Scholar] [Publisher Link]

[4] Norman R. Stoll, "This Wormy World," *Journal of Parasitology*, vol. 33, no. 1, pp. 1-18, 1947. [Google Scholar] [Publisher Link]

[5] Peter J. Hotez et al., "Helminth Infections: The Great Neglected Tropical Diseases," *Journal of Clinical Investigation*, vol. 118, no. 4, pp. 1311-1321, 2008. [CrossRef] [Google Scholar] [Publisher Link]

[6] Pascal Del Giudice et al., "Autochthonous Cutaneous Larva Migrans in France and Europe," *Acta Dermato-Venereologica*, vol. 99, no. 9, pp. 805-808, 2019. [CrossRef] [Google Scholar] [Publisher Link]

[7] A. Jardim-Botelho et al., "Hookworm, Ascaris Lumbricoides Infection and Polyparasitism Associated with Poor Cognitive Performance in Brazilian Schoolchildren," *Tropical Medicine and International Health*, vol. 13, no. 8, pp. 994-1004, 2008. [CrossRef] [Google Scholar] [Publisher Link]

[8] Smita Gupta et al., "Balantidium Coli: Rare Urinary Pathogen or Fecal Contaminant in Urine? Case Study and Review," *IOSR Journal of Dental and Medical Sciences*, vol. 16, no. 3, pp. 88-90, 2017. [CrossRef] [Google Scholar] [Publisher Link]

[9] Fazly Ann Zainalabidin et al., "Monieziasis in Domestic Ruminants in Perak, Malaysia," *Songklanakarin Journal of Science and Technology*, vol. 43, no. 1, pp. 218-221, 2021. [CrossRef] [Google Scholar] [Publisher Link]

[10] Sara Lustigman et al., "A Research Agenda for Helminth Diseases of Humans: The Problem of Helminthiases," *Plos Neglected Tropical Diseases*, vol. 6, no. 4, pp. 1-13, 2012. [CrossRef] [Google Scholar] [Publisher Link]

[11] Martin K. Nielsen, Craig R. Reinemeyer, and Debra C. Sellon, *Chapter 57 – Nematodes*, Equine Infectious Diseases, Elsevier, pp. 475-489, 2014. [CrossRef] [Google Scholar] [Publisher Link]

[12] A. Fenwick, "The Global Burden of Neglected Tropical Diseases," *Public Health*, vol. 126, no. 3, pp. 233-236, 2012. [CrossRef] [Google Scholar] [Publisher Link]

[13] K.M. Faizullah Fuhad et al., "Deep Learning Based Automatic Malaria Parasite Detection from Blood Smear and its Smartphone Based Application," *Diagnostics*, vol. 10, no. 5, pp. 1-22, 2020. [CrossRef] [Google Scholar] [Publisher Link]

[14] John A. Quinn et al., "Deep Convolutional Neural Networks for Microscopy-Based Point of Care Diagnostics," *Proceedings of the 1st Machine Learning for Healthcare Conference*, vol. 56, pp. 271-281, 2016. [Google Scholar] [Publisher Link]

[15] Anson Simon et al., "Shallow CNN with LSTM Layer for Tuberculosis Detection in Microscopic Image," *International Journal of Recent Technology and Engineering*, vol. 7, no. 3, pp. 1-5, 2019. [Google Scholar] [Publisher Link]

[16] Erdal Tasci, Caner Uluturk, and Aybars Ugur, "A Voting-Based Ensemble Deep Learning Method Focusing on Image Augmentation and Preprocessing Variations for Tuberculosis Detection," *Neural Computing and Applications*, vol. 33, no. 22, pp. 15541-15555, 2021. [CrossRef] [Google Scholar] [Publisher Link]

[17] Yaning Li et al., "A Low-Cost, Automated Parasite Diagnostic System Via a Portable, Robotic Microscope and deep Learning," *Journal of Biophotonics*, vol. 12, no. 9, 2019. [CrossRef] [Google Scholar] [Publisher Link]

[18] Gargi Sharma, and Gourav Shrivastava, "Crop Disease Prediction Using Deep Learning Techniques - A Review," *SSRG International Journal of Computer Science and Engineering*, vol. 9, no. 4, pp. 23-28, 2022. [CrossRef] [Google Scholar] [Publisher Link]

[19] Carla Parra et al., "Automatic Identification of Intestinal Parasites in Reptiles Using Microscopic Stool Images and Convolutional Neural Networks," *Plos One*, vol. 17, no. 8, pp. 1-24, 2022. [CrossRef] [Google Scholar] [Publisher Link]

[20] Wei Liu et al., "SSD: Single Shot MultiBox Detector," *European Conference on Computer Vision*, pp. 21-37, 2016. [CrossRef] [Google Scholar] [Publisher Link]

[21] Ghaeth Safar, Mohamad Galiya, and Hassan Salman, "Gyrodactylus Worms of Monogenea Parasitizing on Common Carp Fish in Salah-ALdeen Dam Lake - Lattakia - Syria," *SSRG International Journal of Agriculture and Environmental Science*, vol. 6, no. 5, pp. 41-43, 2019. [CrossRef] [Google Scholar] [Publisher Link]

[22] Joseph Redmon et al, "You Only Look Once: Unified, Real-Time Object Detection," *2016 IEEE Conference on Computer Vision and Pattern Recognition (CVPR)*, pp. 779-788, 2016. [CrossRef] [Google Scholar] [Publisher Link]

[23] L. Kourkouta et al., "Treatment of Avian Influenza," *SSRG International Journal of Nursing and Health Science*, vol. 5, no. 3, pp. 9-11, 2019. [CrossRef] [Publisher Link]

[24] Yanfen Li et al., "A deep Learning-Based Hybrid Framework for Object Detection and Recognition in Autonomous Driving," *IEEE Access*, vol. 8, pp. 194228-194239, 2020. [CrossRef] [Google Scholar] [Publisher Link]

[25] Alexey Bochkovskiy, Chien-Yao Wang, and Hong-Yuan Mark Liao, "YOLOv4: Optimal Speed and Accuracy of Object Detection," *arXiv*, pp. 1-17, 2020. [CrossRef] [Google Scholar] [Publisher Link]